Adenosine Monophosphate-Activated Protein Kinase Activation, Substrate Transporter Translocation, and Metabolism in the Contracting Hyperthyroid Rat Heart

Adenosine Monophosphate-Activated Protein Kinase Activation, Substrate Transporter Translocation, and Metabolism in the Contracting Hyperthyroid Rat Heart

Lisa C. Heather, Mark A. Cole, Helen J. Atherton, Will A. Coumans, Rhys D. Evans, Damian J. Tyler, Jan F. C. Glatz, Joost J. F. P. Luiken, and Kieran Clarke

Cardiac Metabolism Research Group (L.C.H., M.A.C., H.J.A., R.D.E., D.J.T., K.C.), Department of Physiology, Anatomy, and Genetics, University of Oxford, Oxford OX1 3PT, United Kingdom; and Department of Molecular Genetics (W.A.C., J.F.C.G., J.J.F.P.L.), Cardiovascular Research Institute Maastricht (CARIM), Maastricht University, 6200 MD Maastricht, The Netherlands

Thyroid hormones can modify cardiac metabolism via multiple molecular mechanisms, yet their integrated effect on overall substrate metabolism is poorly understood. Here we determined the effect of hyperthyroidism on substrate metabolism in the isolated, perfused, contracting rat heart. Male Wistar rats were injected for 7 d with T_3 (0.2 mg/kg · d ip). Plasma free fatty acids increased by 97%, heart weights increased by 33%, and cardiac rate pressure product, an indicator of contractile function, increased by 33% in hyperthyroid rats. Insulin-stimulated glycolytic rates and lactate efflux rates were increased by 33% in hyperthyroid rat hearts, mediated by an increased insulin-stimulated translocation of the glucose transporter GLUT4 to the sarcolemma. This was accompanied by a 70% increase in phosphorylated AMP-activated protein kinase (AMPK) and a 100% increase in phosphorylated acetyl CoA carboxylase, confirming downstream signaling from AMPK. Fatty acid oxidation rates increased in direct proportion to the increased heart weight and rate pressure product in the hyperthyroid heart, mediated by synchronized changes in mitochondrial enzymes and respiration. Protein levels of the fatty acid transporter, fatty acid translocase (FAT/CD36), were reduced by 24% but were accompanied by a 19% increase in the sarcolemmal content of fatty acid transport protein 1 (FATP1). Thus, the relationship between fatty acid metabolism, cardiac mass, and contractile function was maintained in the hyperthyroid heart, associated with a sarcolemmal reorganization of fatty acid transporters. The combined effects of T_3-induced AMPK activation and insulin stimulation were associated with increased sarcolemmal GLUT4 localization and glycolytic flux in the hyperthyroid heart. (***Endocrinology*** **24: 422–431, 2010)**

Thyroid hormones are key regulators of cardiac physiology. Elevated concentrations of thyroid hormone increase cardiac function and induce cardiac hypertrophy, adaptations that allow the heart to respond to increased peripheral circulatory demand (1–4). Thyroid hormones also increase adipose lipolysis and elevate plasma free fatty acids, consequently altering the supply of substrates available to the heart for energy metabolism (5, 6).

Thyroid hormones can regulate cardiac metabolism via multiple molecular mechanisms (7–11). A number of metabolic proteins are modified in the hyperthyroid heart, including the glucose transporters (GLUT) 1 and 4, pyruvate dehydrogenase kinase 4 (PDK4) and carnitine palmi-

ISSN Print 0013-7227 ISSN Online 1945-7170
Printed in U.S.A.

doi: 10.1210/en.2009-0593 Received May 22, 2009. Accepted October 14, 2009.
First Published Online November 25, 2009

Abbreviations: ACC, Acetyl CoA carboxylase; AMPK, AMP-activated protein kinase; CaMKKβ, calcium/calmodulin-dependent protein kinase kinase-β; CoA, coenzyme A; FABP, fatty acid-binding protein; FAT/CD36, fatty acid translocase; FABPpm, plasma membrane FABP; FATP, fatty acid transport protein; GLUT, glucose transporter; H-FABP, heart-type FABP; IFM, interfibrillar mitochondria; KH, Krebs-Henseleit; MCAD, medium-chain acyl-CoA dehydrogenase; PGC1α, PPAR-γ coactivator 1α; PPAR, peroxisome proliferator-activated receptor; RPP, rate pressure product; SSM, subsarcolemmal mitochondria.

toyltransferase 1 (CPT1) (12–15). Whether these protein changes are sufficient to affect overall substrate metabolism is currently unclear, because studies into fatty acid and glucose metabolism in the hyperthyroid heart have generated conflicting data, with results from cardiomyocytes conflicting with results from ventricular homogenates and intact organs (12, 15–17). In the healthy contracting heart, 60–70% of the ATP for contractile function is generated from the oxidation of fatty acids, with the remainder from the metabolism of carbohydrates (18, 19). Given that thyroid hormones increase contractile function (1), this increased ATP demand would be expected to be accompanied by concomitant changes in substrate metabolism. Because of the interrelationship between metabolism and contraction, measuring substrate metabolism in the intact contracting heart perfused with physiological substrates may most accurately represent metabolism in the *in vivo* hyperthyroid state.

Cardiac substrate metabolism can be regulated at multiple levels by changes in proteins located within mitochondria, in the cytosol, and at the sarcolemma. Sarcolemmal substrate transporters are the initial sites of metabolic control in the heart, because they determine the rate of substrate entry into the cardiomyocyte (20). GLUT1 and -4 control the rate of glucose uptake into the cardiomyocyte, and similarly, the fatty acid transporters, fatty acid translocase (FAT/CD36), fatty acid transport proteins (FATP), and fatty acid-binding proteins (FABP) control the rate of entry of fatty acids. The activity of these transporters can be regulated chronically by altering their transcription or acutely by altering their subcellular location (21). Translocation of substrate transporters from cytosolic vesicles to the sarcolemma acutely increases substrate uptake and can be induced by insulin, contraction, and activation of AMP-activated protein kinase (AMPK) (22–24). At present, it is unclear whether changes in sarcolemmal substrate transporters are key sites of metabolic regulation in the hyperthyroid heart.

Therefore, to investigate the effect of hyperthyroidism on cardiac substrate metabolism, rats were made hyperthyroid over 7 d using T_3, and rates of fatty acid oxidation, myocardial lipid incorporation, and glycolysis were measured in the isolated perfused heart. These results were complemented with measurements of mitochondrial respiration, sarcolemmal substrate transporters, and metabolic regulators to investigate the mechanisms involved in metabolic modulation. Our results demonstrate that fatty acid metabolic rates increased in direct proportion to increased cardiac mass and contractile function in the hyperthyroid heart, associated with a reorganization of fatty acid transporters at the sarcolemma. In addition, insulin-stimulated glycolytic rates were elevated and related to phosphorylation of AMPK and increased GLUT4 sarcolemmal translocation.

Materials and Methods

T_3 administration

Male Wistar rats (~300 g, n = 33) were obtained from a commercial breeder (Harlan, Bicester, UK) and all procedures were in accordance with the United Kingdom Home Office guidelines under The Animals (Scientific Procedures) Act, 1986. T_3 (0.2 mg/kg body weight · d; Sigma, Poole, UK) was dissolved in 0.1 M NaOH and 0.9% (wt/vol) sodium chloride solution (pH 9.5), and injected into the ip cavity, at the same time for 7 consecutive days. Weight-matched controls were injected with 0.9% (wt/vol) sodium chloride solution (pH 9.5). Animals were fasted overnight after the final injection to normalize their metabolic status.

Isolated heart perfusion

Hyperthyroid and control rats were terminally anesthetized, and hearts were excised and perfused in the Langendorff mode at a constant perfusion pressure of 100 mm Hg and an end-diastolic pressure of 4 mm Hg, according to our published protocol (25). Cardiac function was measured using a fluid-filled PVC balloon, inserted into the left ventricle, and attached to a bridge amplifier (AD Instruments, Oxfordshire, UK) and PowerLab data acquisition system. Left ventricular developed pressure was determined as end-systolic minus end-diastolic pressure. Rate pressure product (RPP) was calculated as the product of developed pressure and heart rate and is expressed per heart.

Hearts were perfused with 250 ml recirculating Krebs-Henseleit (KH) buffer (118 mM NaCl, 5 mM KCl, 1.2 mM $MgSO_4$, 1.3 mM $CaCl_2$, 0.5 mM EDTA, 25 mM $NaHCO_3$, 1.2 mM KH_2PO_4, and 11 mM glucose) containing 1.5% (wt/vol) fatty acid-free BSA (Sigma) bound to palmitate. For measurement of palmitate oxidation rates, KH buffer was supplemented with 0.2 μCi/ml [9,10-^{3}H]palmitate (Amersham, Chalfont St. Giles, UK) and 0.5 mM palmitate, followed by 1.0 mM palmitate to maximally stimulate fatty acid metabolism. For measurement of basal glycolytic rates, a separate group of hearts were perfused with KH buffer supplemented with 0.5 mM palmitate and 0.16 μCi/ml D-[2-^{3}H]glucose (Amersham), followed by 3 U/liter insulin to maximally stimulate glycolysis. Coronary flow rates were measured throughout the perfusion protocol and are expressed per heart.

Measurement of metabolic rates

Palmitate oxidation rates were determined by the conversion of [^{3}H]palmitate to ^3H_2O in timed perfusion aliquots (26). Glycolytic rates were determined by the conversion of [^{3}H]glucose to ^3H_2O in timed aliquots (26). Lactate efflux rates were measured in the timed aliquots using lactate dehydrogenase. Myocardial lipid incorporation rates and triglyceride synthesis rates were measured in [^{3}H]palmitate perfused hearts, according to the published protocol (27). Briefly, lipids were extracted from frozen left ventricle using Folch extraction and separated by thin-layer chromatography using a hexane-diethylether-acetic acid aqueous phase. Lipids were visualized with rhodamine 6G under UV light and counted for ^{3}H (25). The specific triglyceride band was identified using internal standards.

Mitochondrial isolation and respiration

Subsarcolemmal mitochondria (SSM) and interfibrillar mitochondria (IFM) were isolated from the left ventricle of a separate group of unperfused hearts according to Palmer *et al.* (28), using a modified Chappell-Perry buffer [100 mM KCl, 50 mM MOPS, 5 mM $MgSO_4 \cdot 7H_2O$, 1 mM EDTA, 1 mM ATP, 0.2% BSA (pH 7.4)]. SSM were isolated by polytron and Potter-Elvejhem homogenization, and IFM were isolated by trypsin digestion [5 mg/g wet weight (gww)] and further homogenization.

Mitochondrial respiration was measured using a Clark-type oxygen electrode (Strathkelvin, Glasgow, UK). Mitochondria were incubated in respiratory medium (100 mM KCl, 50 mM MOPS, 1 mM EGTA, 5 mM KH_2PO_4, 1 mg/ml BSA, pH 7.4) (28), and respiration was measured using palmitoyl CoA with malate and carnitine to assess fatty acid respiration, and pyruvate with malate to assess pyruvate respiration, an indicator of glucose oxidation. State 3 (100 nmol ADP-stimulated) respiration, ADP-maximally stimulated (1000 nmol) respiration, state 4 (ADP-limited) respiration, and ADP/O ratios (ADP phosphorylated per oxygen atom consumed) were measured as previously described (29).

Tissue assays

Tissue assays were performed on freeze-clamped whole cardiac tissue after perfusion. Medium-chain acyl-CoA dehydrogenase (MCAD) activity, a marker of β-oxidation activity, was measured according to the method of Lehman *et al.* (30). Citrate synthase activity, a marker of Krebs cycle activity, was measured according to the method of Srere (31). Glycogen content was determined by the conversion of glycogen to glycosyl units, using amyloglucosidase. Protein concentration was determined using a BCA protein assay reagent kit (Pierce, Rockford, IL). Subcellular fractionation for the determination of intracellular trafficking was carried out according to the established method of Luiken *et al.* (32), to separate the sarcolemma from the intracellular low-density microsomes. Sarcolemmal fractions were confirmed by 3-fold higher levels of Na^+K^+ ATPase, compared with low-density microsome fractions. In addition, low-density microsome fractions had 9-fold higher levels of Rab4 (rat sarcoma superfamily of small GTPases), compared with the sarcolemma (data not shown).

Western blotting

The same concentration of protein from each heart was loaded onto 12.5% SDS-PAGE gels, separated by electrophoresis, and transferred onto Immobilon-P membranes (Millipore, Watford, UK) (25). FAT/CD36 was detected with an antibody donated by Dr. Narendra Tandon (Otsuka Maryland Medicinal Laboratories, Rockville, MD). Plasma membrane FABP (FABPpm) was detected using an antibody donated by Dr. Jorge Calles-Escandon (Wake Forest University School of Medicine, Winston-Salem, NC). Prof. Geoff Holman (University of Bath, Bath, UK) donated the antibody to GLUT4. Antibodies against GLUT1, FATP1, and peroxisome proliferator-activated receptor (PPAR)-γ coactivator 1α (PGC1α) were purchased from Santa Cruz Biotechnology (Santa Cruz, CA), and heart-type FABP (H-FABP also called cFABP) was purchased from Abcam (Cambridge, UK). Antibodies raised against AMPKα, phospho-AMPK (Thr172), and phospho-acetyl CoA carboxylase (ACC) (Ser79) were purchased from Cell Signaling Technology (Beverly, MA) and Upstate (Chandlers Ford, UK), respectively. Even protein loading and transfer were confirmed by Ponceau staining, and protein levels were related to internal standards to ensure homogeneity between samples and gels. Bands were quantified using UN-SCAN-IT gel software (Silk Scientific, Orem, UT), and all samples were run in duplicate on separate gels to confirm results.

Plasma metabolites

Analyses of plasma metabolites were carried out using an automated spectrophotometric analyzer (Monarch Laboratories, Lexington, KT). Plasma insulin was determined by enzyme-linked immunosorbent assay (Mercodia, Uppsala, Sweden).

Statistical analysis

Results are presented as means ± SEM and were analyzed using an unpaired *t* test. Perfusion data were analyzed using repeated-measures ANOVA followed by paired or unpaired *t* tests where appropriate (SPSS 12.0 for Windows). Results were considered significant at $P < 0.05$.

Results

Physical characteristics

Administration of T_3 for 7 d caused a 9% decrease in body weight compared with control rats (Table 1). T_3 induced significant cardiac hypertrophy, because heart weights were increased by 33% in hyperthyroid rats compared with controls. Epididymal fat pad weight, an indicator of adiposity, was decreased by 44% in hyperthyroid rats compared with controls. In comparison with controls, hyperthyroid rats had a 97% increase in plasma free fatty acid concentrations (Table 1). There were no other significant differences in plasma metabolite concentrations between control and hyperthyroid rats.

Cardiac function

Cardiac function was significantly increased in hyperthyroid hearts compared with control hearts (Table 2).

TABLE 1. Physical characteristics and fasting plasma metabolite concentrations in control and hyperthyroid rats

	Control (n = 13)	Hyperthyroid (n = 12)
Physical characteristics		
Initial body weight (g)	307 ± 5	308 ± 4
Final body weight (g)	303 ± 6	276 ± 5[a]
Heart weight (g)	1.26 ± 0.03	1.67 ± 0.06[a]
Epididymal fat pad weight (g)	4.23 ± 0.73	2.36 ± 0.26[a]
Plasma metabolites		
Free fatty acids (mmol/liter)	0.36 ± 0.03	0.71 ± 0.03[a]
Glucose (mmol/liter)	6.11 ± 0.35	5.13 ± 0.42
Lactate (mmol/liter)	2.89 ± 0.38	2.76 ± 0.38
Cholesterol (mmol/liter)	1.34 ± 0.11	1.09 ± 0.10
Insulin (μg/liter)	0.35 ± 0.04	0.35 ± 0.02

[a] $P < 0.05$ *vs.* control. For plasma insulin and epididymal fat pad weight, n = 6 per group.

TABLE 2. Cardiac function in isolated hearts perfused with 0.5 and 1.0 mM palmitate, and under basal and insulin-stimulated conditions, from control and hyperthyroid rats

	Control	Hyperthyroid
0.5 mM palmitate		
Heart rate (beats/min)	289 ± 9	323 ± 13[a]
Developed pressure (mm Hg)	126 ± 3	131 ± 4
RPP (mm Hg/min × 10^3)	37 ± 1	44 ± 2[a]
Coronary flow rates (ml/min)	19 ± 1	21 ± 1
1.0 mM palmitate		
Heart rate (beats/min)	289 ± 14	322 ± 12
Developed pressure (mm Hg)	129 ± 4	145 ± 4[a,b]
RPP (mm Hg/min × 10^3)	38 ± 1	48 ± 2[a,b]
Coronary flow rates (ml/min)	18 ± 1	21 ± 1[a]
Basal		
Heart rate (beats/min)	289 ± 8	368 ± 24[a]
Developed pressure (mm Hg)	135 ± 5	121 ± 7
RPP (mm Hg/min × 10^3)	40 ± 1	45 ± 1[a]
Coronary flow rates (ml/min)	19 ± 1	24 ± 1[a]
Insulin-stimulated		
Heart rate (beats/min)	294 ± 9	369 ± 18[a]
Developed pressure (mm Hg)	126 ± 5	138 ± 7[c]
RPP (mm Hg/min × 10^3)	39 ± 1	52 ± 2[a,c]
Coronary flow rates (ml/min)	19 ± 1	25 ± 1[a,c]

Data are expressed per heart.

[a] $P < 0.05$ *vs.* control group under the same perfusion conditions; [b] $P < 0.05$ *vs.* hyperthyroid perfused with 0.5 mM palmitate; [c] $P < 0.05$ *vs.* hyperthyroid perfused under basal conditions. n = 5–7.

Both heart rate and developed pressure were increased after 7 d T_3 administration. This resulted in RPP being significantly increased by 13–33% in hyperthyroid hearts, compared with controls under all perfusion conditions. When the availability of substrate to the hearts was increased, either with 1.0 mM palmitate or with insulin, RPP increased further in hyperthyroid hearts but not in control hearts. Increased cardiac function in hyperthyroid hearts was accompanied by a proportional significant increase in coronary flow rates, compared with controls.

Cardiac fatty acid oxidation and myocardial lipid incorporation rates

Fatty acids are the predominant substrate used by the contracting heart to produce ATP (19). At both 0.5 and 1.0 mM palmitate, rates of palmitate oxidation per gww were not significantly different between control and hyperthyroid hearts (Fig. 1). As T_3 induced an increase in cardiac mass, palmitate oxidation rates per heart were significantly increased in hyperthyroid hearts by 29% when perfused with at 0.5 mM palmitate (0.24 μmol/min · heart in control hearts *vs.* 0.31 μmol/min · heart in hyperthyroid hearts, $P < 0.05$) and by 32% when perfused with 1.0 mM palmitate (0.31 μmol/min · heart in control hearts *vs.* 0.41 μmol/min · heart in hyperthyroid hearts, $P < 0.05$), compared with controls. As contractile function was also increased in the perfused hyperthyroid

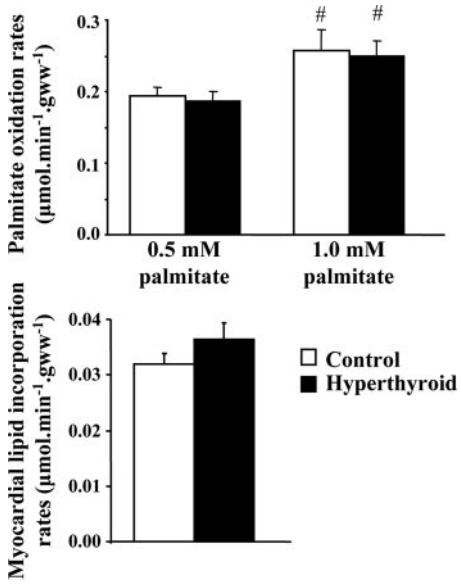

FIG. 1. *Top*, Fatty acid oxidation rates in isolated hearts from control and hyperthyroid rats, perfused with 0.5 and 1.0 mM palmitate; *bottom*, myocardial lipid incorporation rates in control and hyperthyroid rat hearts. #, $P < 0.05$ *vs.* 0.5 mM palmitate rates. Control n = 6; hyperthyroid n = 7.

hearts, palmitate oxidation rates per heart were normalized to RPP to determine whether changes in metabolism were related to changes in cardiac work. Hyperthyroid hearts oxidized the same amount of fatty acid per unit work at 0.5 mM palmitate (6.5 ± 0.4 pmol/mm Hg in control hearts *vs.* 7.0 ± 0.6 pmol/mm Hg in hyperthyroid hearts) and 1.0 mM palmitate (8.2 ± 0.5 pmol/mm Hg in control hearts *vs.* 8.4 ± 0.4 pmol/mm Hg in hyperthyroid hearts) as control hearts. Thus, palmitate oxidation rates increased in direct proportion to increased cardiac mass and contractile function in hyperthyroid hearts.

Rates of myocardial lipid incorporation into the myocardial lipid storage pool were not significantly different per gww between control and hyperthyroid hearts. In addition, myocardial triacylglycerol synthesis rates were not significantly different between groups, with 23 ± 2 nmol/min · gww in control hearts and 22 ± 3 nmol/min · gww in hyperthyroid hearts. Total palmitate utilization is the sum of palmitate oxidation and myocardial lipid incorporation and is an indirect measure of fatty acid uptake (25, 27). Total palmitate utilization rates per gww were not significantly different between control and hyperthyroid hearts (0.26 ± 0.02 μmol/gww · min in control hearts *vs.* 0.26 ± 0.02 μmol/gww · min in hyperthyroid hearts). As heart weights were increased by 33% in hyperthyroid rats, there was a proportional increase in total palmitate utilization to maintain the same rate per gww, thereby maintaining the relationship between fatty acid metabolism and cardiac mass in the hyperthyroid heart.

TABLE 3. Respiration rates in SSM and IFM isolated from control and hyperthyroid hearts, using palmitoyl CoA and pyruvate as substrates

	SSM		IFM	
	Control	**Hyperthyroid**	**Control**	**Hyperthyroid**
Yield (mg/gww)	4.8 ± 0.3	5.2 ± 0.1	10.2 ± 1.8	9.2 ± 1.0
Palmitoyl CoA				
State 3	90 ± 8	97 ± 7	129 ± 18	157 ± 15
Maximal ADP	127 ± 14	126 ± 14	183 ± 32	214 ± 25
ADP/O	2.18 ± 0.25	2.35 ± 0.28	2.16 ± 0.18	2.53 ± 0.15
State 4	26 ± 3	29 ± 4	31 ± 3	45 ± 1[a]
Pyruvate				
State 3	115 ± 16	123 ± 10	161 ± 10	180 ± 17
Maximal ADP	132 ± 15	132 ± 11	212 ± 17	212 ± 21
ADP/O	2.87 ± 0.08	2.82 ± 0.14	2.91 ± 0.14	2.76 ± 0.18
State 4	30 ± 1	36 ± 2[a]	34 ± 1	50 ± 3[a]

Respiration rates are expressed as nanomoles O_2 per minute per milligram mitochondrial protein.

[a] $P < 0.05$ *vs.* control under the same conditions; n = 4 per group.

Mitochondrial fatty acid utilization

We next investigated the effect of hyperthyroidism on isolated mitochondrial fatty acid respiration. The yields of SSM and IFM per gww of cardiac tissue were not significantly different between control and hyperthyroid hearts (Table 3). Thus, as heart weight increased, there was a proportional increase in mitochondrial content. Palmitoyl CoA-dependent state 3 respiration rates and maximal ADP-stimulated respiration rates were not significantly different in either SSM or IFM between control and hyperthyroid hearts. ADP/O ratios with palmitoyl CoA were also not significantly different between groups. Thus, mitochondrial ADP-stimulated fatty acid respiration rates were in agreement with the maintained fatty acid oxidation rates per gww in the hyperthyroid perfused hearts (Fig. 1). In contrast, state 4 respiration rates, measured under nonphosphorylating conditions, were increased by 45% in IFM from hyperthyroid hearts compared with controls (Table 3).

Fatty acid metabolism enzymes and protein levels

We investigated whether the enzymes and proteins involved in regulating cardiac fatty acid metabolic flux were changed by hyperthyroidism. Total cardiac protein concentrations were the same between groups (94 ± 6 mg/gww in control hearts *vs.* 107 ± 5 mg/gww in hyperthyroid hearts). PGC1α protein levels were not significantly different between control and hyperthyroid hearts, indicating no change in mitochondrial biogenesis per milligram protein, in agreement with the maintained mitochondrial yield (Fig. 2). MCAD activity, a marker of β-oxidation and a PPARα-regulated enzyme, was not significantly different per gww between groups. In addition, citrate synthase activity, a marker of Krebs cycle activity, was similar per gww between control and hyperthyroid hearts. Protein levels of the cytosolic H-FABP were the same between groups, indicating no gross change in the capacity for intracellular trafficking of fatty acids.

Total protein levels of the fatty acid transporters FABPpm and FATP1 were the same per milligram protein between control and hyperthyroid hearts (Fig. 2). However, total protein levels of the fatty acid transporter FAT/CD36 were 24% lower in hyperthyroid hearts compared with controls. Given the normal rates of fatty acid utilization in the hyperthyroid hearts, the decrease in total FAT/CD36 levels was unexpected. Therefore, subcellular fractionation was performed to measure the amount of fatty acid transporters present at the sarcolemma, directly regulating the rate of fatty acid uptake (21, 33). Sarcolemmal FABPpm content was not significantly different between groups, with 47 ± 2% at the sarcolemma in control hearts and 46 ± 4% at the sarcolemma in hyperthyroid hearts. The percentage distribution of FAT/CD36 was not significantly different between groups with 42 ± 3% at the sarcolemma in control hearts and 37 ± 1% at the sarcolemma in hyperthyroid hearts. However, because total cellular levels of FAT/CD36 were reduced by 24%, the absolute amount of FAT/CD36 at the sarcolemma in hyperthyroid hearts was 33% lower than control hearts (1.00 ± 0.11 in control hearts *vs.* 0.67 ± 0.06 in hyperthyroid hearts, arbitrary units, $P < 0.05$). In contrast, there was a cellular redistribution of FATP1 within the hyperthyroid hearts (Fig. 2). There was a 19% increase in sarcolemmal FATP1 content and a 19% decrease in low-density microsome FATP1 content in hyperthyroid hearts compared with controls, potentially compensating for the decreased sarcolemmal FAT/CD36 to maintain normal rates of fatty acid uptake.

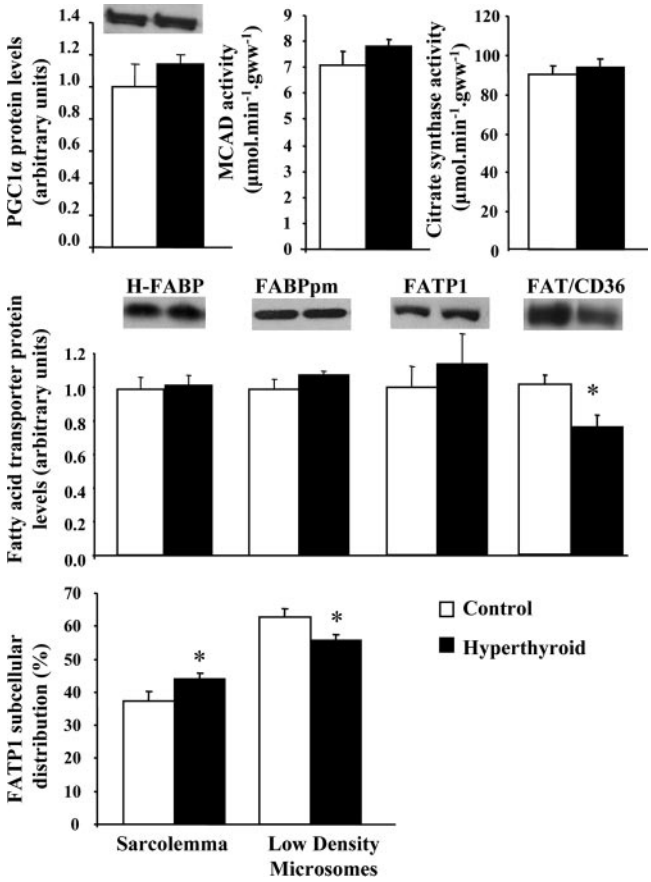

FIG. 2. *Top*, Protein levels of PGC1α and enzyme activities of MCAD and citrate synthase in hearts from control and hyperthyroid rats; *middle*, protein levels of fatty acid transporters H-FABP, FABPpm, FATP1, and FAT/CD36 from control and hyperthyroid rat hearts; *bottom*, subcellular distribution of FATP1 between the sarcolemma and low-density microsomes in control and hyperthyroid rat hearts. Protein levels are expressed in arbitrary units, relative to the normalized control average. Bands shown correspond to molecular masses of PGC1α (90 kDa), H-FABP (15 kDa), FABPpm (40 kDa), FATP1 (63 kDa), and FAT/CD36 (88 kDa). *, $P < 0.05$ *vs.* control. n = 5–6 per group.

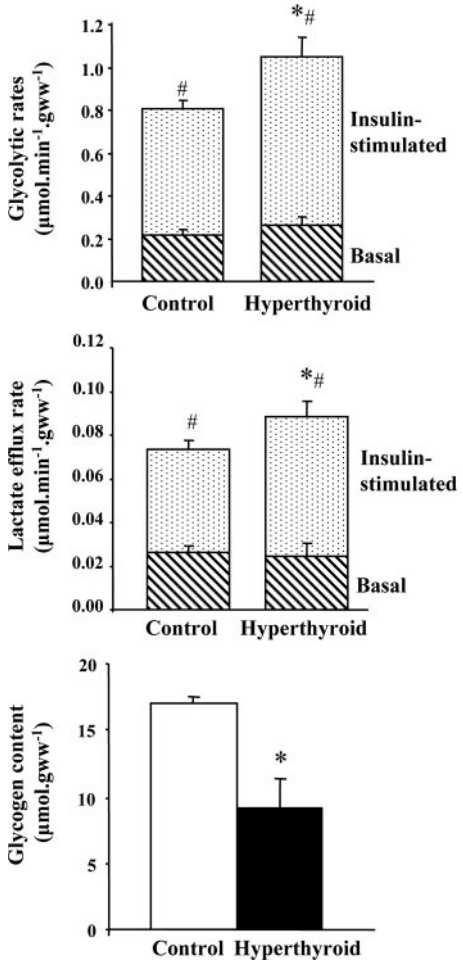

FIG. 3. *Top* and *middle*, Glycolytic rates (*top*) and lactate efflux rates (*middle*) in isolated hearts from control and hyperthyroid rats, perfused under basal and insulin-stimulated conditions; *bottom*, glycogen concentrations from control and hyperthyroid hearts after insulin stimulation. *, $P < 0.05$ *vs.* control; #, $P < 0.05$ *vs.* basal rates. Control n = 7; hyperthyroid n = 5.

Glycolytic rates

Our second question was whether hyperthyroidism had a significant effect on cardiac glucose metabolism. Basal glycolytic rates were measured in perfused hearts in the absence of insulin and were not significantly different per gww between control and hyperthyroid hearts (Fig. 3). However, when hearts were stimulated with insulin, rates of glycolysis were significantly increased by 33% per gww in hyperthyroid hearts compared with controls, in excess of the increased cardiac mass and contractile function. Under basal perfusion conditions, cardiac lactate efflux rates were comparable between groups. However, lactate efflux rates under insulin-stimulated conditions were significantly increased by 33% per gww in hyperthyroid hearts compared with controls. Myocardial glycogen content was measured after insulin-stimulated perfusion and was decreased by 46% in the hyperthyroid hearts compared with control hearts. Thus, increased insulin sensitivity in hyperthyroid hearts was selectively diverting glucose through glycolysis.

Mitochondrial pyruvate utilization

Mitochondrial pyruvate oxidation was measured to determine whether hyperthyroidism modified the ability to oxidize the end-product of glycolysis. Pyruvate respiration rates under state 3 conditions and maximal ADP-stimulated respiration rates were not significantly different in SSM and IFM between hyperthyroid and control hearts (Table 3). ADP/O ratios were not significantly different between groups respiring with pyruvate. Thus, under phosphorylating conditions, mitochondrial pyruvate respiration, an indicator of glucose oxidation, was similar in control and hyperthyroid hearts, in agreement with the mitochondrial fatty acid respiration rates. However, state 4 pyruvate respiration rates were increased by 20 and 47% in SSM and IFM from hyperthyroid hearts, respectively.

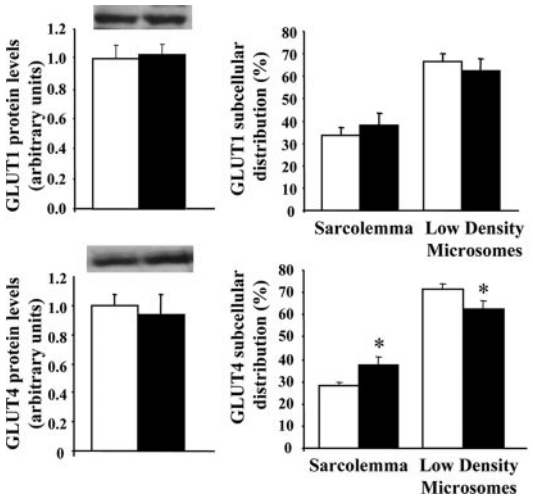

FIG. 4. GLUT1 and GLUT4 protein levels, and percentage distribution between sarcolemma and low-density microsome fractions, after insulin stimulation of hearts from control and hyperthyroid rats. Protein levels are expressed in arbitrary units, relative to the normalized control average. Bands shown correspond to molecular masses of GLUT1 (55 kDa) and GLUT4 (50 kDa). *, $P < 0.05$ *vs.* control. n = 5–6 per group.

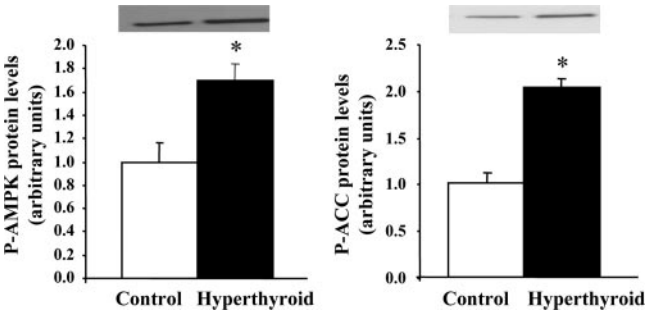

FIG. 5. Phosphorylated AMPK and ACC protein levels from control and hyperthyroid rat hearts. Protein levels are expressed in arbitrary units, relative to the normalized control average. Bands shown correspond to molecular masses of phospho (P)-AMPK (62 kDa) and P-ACC (257 kDa). Control n = 7; hyperthyroid n = 5.

Glucose Transporters

We hypothesized that increased insulin-stimulated glycolytic rates in hyperthyroid hearts were due to changes in sarcolemmal glucose transport. Both GLUT1 and GLUT4 total protein levels were not significantly different per milligram protein between control and hyperthyroid hearts (Fig. 4). GLUT1 subcellular distribution was not significantly different between groups after insulin stimulation, with a similar percentage at the sarcolemma in control and hyperthyroid hearts. In contrast, sarcolemmal GLUT4 content was significantly increased by 33% in hyperthyroid hearts, and low-density microsomal GLUT4 content decreased by 33% compared with control hearts after insulin stimulation. The increased sarcolemmal GLUT4 content was not present before insulin stimulation, because under basal perfusion conditions, sarcolemmal GLUT4 content was 21 ± 3% in control hearts and 21 ± 5% in hyperthyroid hearts. Thus, in hyperthyroid hearts, there was a greater redistribution of GLUT4 to the sarcolemma after insulin stimulation.

AMPK activation

Increased sarcolemmal GLUT4 content, increased glycolysis, and decreased glycogen content in our hyperthyroid hearts were similar to the metabolic changes that follow AMPK activation (34). Total AMPKα levels were not significantly different between groups (1.00 ± 0.06 in control hearts *vs.* 1.00 ± 0.03 in hyperthyroid hearts). However, in hyperthyroid hearts, levels of phosphorylated AMPK were increased by 70% compared with control hearts, demonstrating activation of AMPK (Fig. 5). In addition, phosphorylation of the AMPK target protein ACC was increased by 100% compared with control hearts, confirming increased downstream signaling from AMPK in the hyperthyroid heart.

Discussion

T_3 administration for 7 d increased fatty acid oxidation in direct proportion to the increased cardiac mass and contractile function induced in the hyperthyroid heart, accompanied by decreased sarcolemmal FAT/CD36 protein levels and increased sarcolemmal FATP1 protein levels. Glycolytic rates and GLUT4 translocation to the sarcolemma were increased under insulin-stimulated conditions, associated with phosphorylation of AMPK and phosphorylation of its downstream target ACC in the hyperthyroid heart.

Fatty acid metabolism in the hyperthyroid heart

Fatty acid metabolism was unchanged per gww in the perfused, contracting hyperthyroid heart, with no significant differences in fatty acid oxidation, lipid incorporation, mitochondrial respiration, or proteins involved in fatty acid oxidation per gww. This is in agreement with Degens *et al.* (17) who found no change in palmitate oxidation rates per gww in left ventricular homogenates from hyperthyroid rats and no change in mRNA levels of fatty acid oxidation genes. To allow direct comparison with controls, metabolic rates were expressed per gww of heart tissue. However, when these data were expressed in relation to total cardiac mass and cardiac function, it demonstrated additional information obtained by measuring metabolism in an intact heart under physiological, contracting conditions. When perfused with 1.0 mM palmitate, fatty acid oxidation rates were unchanged per gww, and combined with the 33% increase in heart wet weight, this resulted in fatty acid oxidation rates per heart increasing by 30%. When rates of fatty acid oxidation per heart were normalized to the 26% increase in RPP, the data

revealed that hyperthyroid hearts oxidized the same amount of fatty acid per unit work as control hearts. Therefore, as cardiac function and mass were increased by the action of T_3, there was a proportional increase in fatty acid metabolism. Studies in hyperthyroid patients have reported left ventricular hypertrophy and increased cardiac output, accompanied by increased oxidative metabolism at the whole organ level (3, 4, 35), indicating a similar interrelationship between metabolism and function as in our hyperthyroid rats. These data are consistent with long-chain fatty acids being the primary substrate used by the heart to power contraction (18, 19); thereby, increased fatty acid metabolism in hyperthyroidism would supply additional ATP for the increased workload placed on the heart. Thus, thyroid hormones must induce synchronized changes in multiple molecular pathways involved in metabolism and contraction to maintain the relationship between these two factors in the hyperthyroid heart.

Fatty acids are potent PPARα agonists, yet despite a near doubling of plasma free fatty acid concentrations in our hyperthyroid rats, there was no increase in MCAD activity, a key PPARα-responsive enzyme (36). This unusual response is due to cross talk between thyroid and PPARα signaling pathways, and elegant studies have demonstrated that T_3 signaling actively suppresses PPARα activation in isolated cells (9, 37). The PGC1α transcription factor can also influence fatty acid oxidation via its overall regulation of mitochondrial biogenesis (36), and after 7 d of T_3 treatment, we found no increase in cardiac PGC1α protein levels, in agreement with Irrcher *et al.* (38). Thus, a combination of T_3-mediated PPARα suppression and maintained PGC1α regulation likely contribute to the control of fatty acid oxidation in the hyperthyroid heart.

Fatty acid transporter distribution in the hyperthyroid heart

A number of proteins have been implicated in sarcolemmal fatty acid uptake; these include FAT/CD36, FABPpm, and FATP1 (21). Although the precise mechanism by which these three proteins operate and cooperate remains to be determined, they have each been shown to facilitate fatty acid uptake and to translocate from the low-density microsomes to the sarcolemma in response to stimuli (21, 33). In addition to its critical role in fatty acid uptake, van der Putten *et al.* (39) identified FAT/CD36 as one of a number of proteins implicated in thyroid hormone transport, mediating the uptake of T_3 across the plasma membrane (40). Thus, the decreased FAT/CD36 total protein and sarcolemmal content in our hyperthyroid rats may be to limit excessive uptake of thyroid hormone. However, to maintain cardiac fatty acid uptake rates, the down-regulation of FAT/CD36 required a compensatory increase in another fatty acid transporter, and our data suggest this was achieved by increased sarcolemmal FATP1 content in the hyperthyroid hearts. This compensation of FATP1 for a deficiency in FAT/CD36 has been noted in FAT/CD36 knockout mice, in which FATP1 is up-regulated 1.8-fold in this genetic model (41). Thus, sarcolemmal reorganization of fatty acid transporters likely mediates normal rates of fatty acid uptake in the presence of elevated thyroid hormones.

Increased state 4 respiration in the hyperthyroid heart

State 4 respiration rates, measured under nonphosphorylating conditions, were increased in mitochondria from hyperthyroid hearts. This is due to increased basal leak of protons into the mitochondrial matrix independent of ADP phosphorylation and has been reported previously in cardiac mitochondria from hyperthyroid rats (42). The increased nonphosphorylation state 4 respiration may be attributed to uncoupling proteins 2 and 3 or the adenine nucleotide translocase proteins, all of which are up-regulated by thyroid hormones (42, 43). However, despite the increased state 4 respiration rates, there was no increase in state 3 respiration, maximal ADP-stimulated respiration, or ADP/O ratios, suggesting that the basal leak was not sufficient to affect respiration when mitochondria were metabolically active under phosphorylating conditions. Because the intact heart is constantly active, phosphorylating ADP to ATP, it is difficult to extrapolate the increased state 4 respiration to the contracting organ.

Combined effects of insulin and AMPK on glycolysis

In the hyperthyroid heart, rates of glycolysis per gww were increased under insulin-stimulated conditions, an increase in excess of the cardiac hypertrophy and elevated RPP. Despite the increased insulin-stimulated glycolysis, basal glycolytic rates were not increased, indicating that it was not T_3 *per se* that was enhancing glucose metabolism but a positive interaction between a T_3-activated process and insulin. Increased sarcolemmal GLUT4 content, increased glycolysis and decreased glycogen content are characteristic of the metabolic changes that follow AMPK activation (34), and phosphorylation of AMPK and its downstream target ACC were clearly evident in our hyperthyroid hearts. Jakobsen *et al.* (44) showed that AMPK can selectively phosphorylate the insulin receptor substrate 1 (IRS1) at Ser789. This additional phosphorylation of insulin receptor substrate 1 by AMPK increases insulin signaling to a greater extent than insulin stimulation alone (45–47). Thus, the above mechanism of AMPK-enhanced insulin signaling would account for the increased insulin sensitivity, increased GLUT4 translocation, and increased glycolytic rates in the contracting hyperthyroid heart.

Mechanisms for AMPK activation

AMPK is often described as the cellular fuel gauge, because it is phosphorylated and activated by serine/threonine Kinase11 (LKB1) in response to increased AMP concentrations (48). However, ^{31}P nuclear magnetic resonance spectroscopy data obtained from the perfused hyperthyroid heart show that AMP levels are not elevated and that there is no change in the ATP to ADP ratio, suggesting this may not be the mechanism of activation in the hyperthyroid heart (49, 50). In recent years, alternative mechanisms of AMPK activation have been identified, which operate independently of AMP and LKB1 (48). In LKB1 knockout mice, AMPK phosphorylation occurs via a calcium-dependent activation of calcium/calmodulin-dependent protein kinase kinase-β (CaMKKβ) (51). In addition, in LKB1-deficient HeLa cells, treatment with T_3 significantly increased AMPK activity via elevated calcium and CaMKKβ (52). Therefore, in our perfused contracting hyperthyroid hearts, AMPK activation may occur via elevation of calcium levels and activation of CaMKKβ.

In conclusion, hyperthyroidism increased glycolysis and sarcolemmal GLUT4 levels by the combined effects of AMPK activation and insulin stimulation. Fatty acid oxidation rates increased in direct proportion to increased cardiac mass and contractile function induced in the hyperthyroid heart. This was associated with a reorganization of sarcolemmal fatty acid transporters, because FAT/CD36 protein levels were decreased, potentially to limit uptake of T_3 by this promiscuous transporter, and accompanied by an increase in sarcolemmal FATP1. Thus, cardiac fatty acid and glucose metabolism are modified in hyperthyroidism when measured under physiological conditions in the intact, contracting heart.

Acknowledgments

We thank Narendra Tandon, Jorges Calles-Escandon, and Geoff Holman for their kind donations of primary antibodies. Thanks to Dr. Charles Hoppel, Case Western Reserve University, for assistance with the mitochondrial respiration experiments. Thanks also to Richard P Leoni, Gillian Watson, You-Guo Niu, and Emma Carter for technical assistance.

Address all correspondence and requests for reprints to: Dr. Lisa Heather, Department of Physiology, Anatomy, and Genetics, Sherrington Building, University of Oxford, Parks Road, Oxford OX1 3PT, United Kingdom. E-mail: lisa.heather@dpag.ox.ac.uk.

This work was supported by grants from the British Heart Foundation (RG/07/004/22659), Medical Research Council, British Council, and Platform Beta Techniek.

Disclosure Summary: The authors have nothing to disclose.

References

1. **Beznak M** 1962 Cardiovascular effects of thyroxine treatment in normal rats. Can J Biochem Physiol 40:1647–1654
2. **Trivieri MG, Oudit GY, Sah R, Kerfant BG, Sun H, Gramolini AO, Pan Y, Wickenden AD, Croteau W, Morreale de Escobar G, Pekhletski R, St Germain D, Maclennan DH, Backx PH** 2006 Cardiac-specific elevations in thyroid hormone enhance contractility and prevent pressure overload-induced cardiac dysfunction. Proc Natl Acad Sci USA 103:6043–6048
3. **Dörr M, Wolff B, Robinson DM, John U, Lüdemann J, Meng W, Felix SB, Völzke H** 2005 The association of thyroid function with cardiac mass and left ventricular hypertrophy. J Clin Endocrinol Metab 90:673–677
4. **Martin 3rd WH, Spina RJ, Korte E, Yarasheski KE, Angelopoulos TJ, Nemeth PM, Saffitz JE** 1991 Mechanisms of impaired exercise capacity in short duration experimental hyperthyroidism. J Clin Invest 88:2047–2053
5. **Elks ML, Manganiello VC** 1985 Effects of thyroid hormone on regulation of lipolysis and adenosine 3′,5′-monophosphate metabolism in 3T_3-L1 adipocytes. Endocrinology 117:947–953
6. **Yamamoto N, Li QL, Mita S, Morisawa S, Inoue A** 2001 Inhibition of thyroid hormone binding to the nuclear receptor by mobilization of free fatty acids. Horm Metab Res 33:131–137
7. **Jansen MS, Cook GA, Song S, Park EA** 2000 Thyroid hormone regulates carnitine palmitoyltransferase Iα gene expression through elements in the promoter and first intron. J Biol Chem 275:34989–34997
8. **Bassett JH, Harvey CB, Williams GR** 2003 Mechanisms of thyroid hormone receptor-specific nuclear and extra nuclear actions. Mol Cell Endocrinol 213:1–11
9. **Chu R, Madison LD, Lin Y, Kopp P, Rao MS, Jameson JL, Reddy JK** 1995 Thyroid hormone (T_3) inhibits ciprofibrate-induced transcription of genes encoding β-oxidation enzymes: cross talk between peroxisome proliferator and T_3 signaling pathways. Proc Natl Acad Sci USA 92:11593–11597
10. **Hyyti OM, Ning XH, Buroker NE, Ge M, Portman MA** 2006 Thyroid hormone controls myocardial substrate metabolism through nuclear receptor-mediated and rapid posttranscriptional mechanisms. Am J Physiol Endocrinol Metab 290:E372–E379
11. **Torrance CJ, Usala SJ, Pessin JE, Dohm GL** 1997 Characterization of a low affinity thyroid hormone receptor binding site within the rat GLUT4 gene promoter. Endocrinology 138:1215–1223
12. **De K, Ghosh G, Datta M, Konar A, Bandyopadhyay J, Bandyopadhyay D, Bhattacharya S, Bandyopadhyay A** 2004 Analysis of differentially expressed genes in hyperthyroid-induced hypertrophied heart by cDNA microarray. J Endocrinol 182:303–314
13. **Gosteli-Peter MA, Schmid C, Zapf J** 1996 Triiodothyronine increases glucose transporter isotype 4 mRNA expression, glucose transport, and glycogen synthesis in adult rat cardiomyocytes in long-term culture. Biochem Biophys Res Commun 221:521–524
14. **Holness MJ, Smith ND, Bulmer K, Hopkins T, Gibbons GF, Sugden MC** 2002 Evaluation of the role of peroxisome-proliferator-activated receptor α in the regulation of cardiac pyruvate dehydrogenase kinase 4 protein expression in response to starvation, high-fat feeding and hyperthyroidism. Biochem J 364:687–694
15. **Sugden MC, Priestman DA, Orfali KA, Holness MJ** 1999 Hyperthyroidism facilitates cardiac fatty acid oxidation through altered regulation of cardiac carnitine palmitoyltransferase: studies *in vivo* and with cardiac myocytes. Horm Metab Res 31:300–306
16. **Seymour AM, Eldar H, Radda GK** 1990 Hyperthyroidism results in increased glycolytic capacity in the rat heart. A ^{31}P-NMR study. Biochim Biophys Acta 1055:107–116
17. **Degens H, Gilde AJ, Lindhout M, Willemsen PH, Van Der Vusse GJ, Van Bilsen M** 2003 Functional and metabolic adaptation of the heart to prolonged thyroid hormone treatment. Am J Physiol Heart Circ Physiol 284:H108–H115

18. **Bing RJ, Siegel A, Ungar I, Gilbert M** 1954 Metabolism of the human heart. II. Studies on fat, ketone and amino acid metabolism. Am J Med 16:504–515
19. **van der Vusse GJ, Glatz JF, Stam HC, Reneman RS** 1992 Fatty acid homeostasis in the normoxic and ischemic heart. Physiol Rev 72: 881–940
20. **Stanley WC, Recchia FA, Lopaschuk GD** 2005 Myocardial substrate metabolism in the normal and failing heart. Physiol Rev 85: 1093–1129
21. **Luiken JJ, Coort SL, Koonen DP, van der Horst DJ, Bonen A, Zorzano A, Glatz JF** 2004 Regulation of cardiac long-chain fatty acid and glucose uptake by translocation of substrate transporters. Pflugers Arch 448:1–15
22. **Kurth-Kraczek EJ, Hirshman MF, Goodyear LJ, Winder WW** 1999 5′-AMP-activated protein kinase activation causes GLUT4 translocation in skeletal muscle. Diabetes 48:1667–1671
23. **Bonen A, Luiken JJ, Arumugam Y, Glatz JF, Tandon NN** 2000 Acute regulation of fatty acid uptake involves the cellular redistribution of fatty acid translocase. J Biol Chem 275:14501–14508
24. **Luiken JJ, Coort SL, Koonen DP, Bonen A, Glatz JF** 2004 Signalling components involved in contraction-inducible substrate uptake into cardiac myocytes. Proc Nutr Soc 63:251–258
25. **Heather LC, Cole MA, Lygate CA, Evans RD, Stuckey DJ, Murray AJ, Neubauer S, Clarke K** 2006 Fatty acid transporter levels and palmitate oxidation rate correlate with ejection fraction in the infarcted rat heart. Cardiovasc Res 72:430–437
26. **Lopaschuk GD, Barr RL** 1997 Measurements of fatty acid and carbohydrate metabolism in the isolated working rat heart. Mol Cell Biochem 172:137–147
27. **Hauton D, Bennett MJ, Evans RD** 2001 Utilisation of triacylglycerol and non-esterified fatty acid by the working rat heart: myocardial lipid substrate preference. Biochim Biophys Acta 1533:99–109
28. **Palmer JW, Tandler B, Hoppel CL** 1977 Biochemical properties of subsarcolemmal and interfibrillar mitochondria isolated from rat cardiac muscle. J Biol Chem 252:8731–8739
29. **Heather LC, Carr CA, Stuckey DJ, Pope S, Morten KJ, Carter EE, Edwards LM, Clarke K** 31 Aug 2009 Critical role of complex III in the early metabolic changes following myocardial infarction. Cardiovasc Res 10.1093/cvr/cvp276
30. **Lehman TC, Hale DE, Bhala A, Thorpe C** 1990 An acyl-coenzyme A dehydrogenase assay utilizing the ferricenium ion. Anal Biochem 186:280–284
31. **Srere P** 1969 Citrate synthase. Methods Enzymol 13:3–5
32. **Luiken JJ, Koonen DP, Willems J, Zorzano A, Becker C, Fischer Y, Tandon NN, Van Der Vusse GJ, Bonen A, Glatz JF** 2002 Insulin stimulates long-chain fatty acid utilization by rat cardiac myocytes through cellular redistribution of FAT/CD36. Diabetes 51:3113–3119
33. **Wu Q, Ortegon AM, Tsang B, Doege H, Feingold KR, Stahl A** 2006 FATP1 is an insulin-sensitive fatty acid transporter involved in diet-induced obesity. Mol Cell Biol 26:3455–3467
34. **Kahn BB, Alquier T, Carling D, Hardie DG** 2005 AMP-activated protein kinase: ancient energy gauge provides clues to modern understanding of metabolism. Cell Metab 1:15–25
35. **Bengel FM, Lehnert J, Ibrahim T, Klein C, Bülow HP, Nekolla SG, Schwaiger M** 2003 Cardiac oxidative metabolism, function, and metabolic performance in mild hyperthyroidism: a noninvasive study using positron emission tomography and magnetic resonance imaging. Thyroid 13:471–477
36. **Finck BN, Kelly DP** 2002 Peroxisome proliferator-activated receptor α (PPARα) signaling in the gene regulatory control of energy metabolism in the normal and diseased heart. J Mol Cell Cardiol 34:1249–1257
37. **Miyamoto T, Kaneko A, Kakizawa T, Yajima H, Kamijo K, Sekine R, Hiramatsu K, Nishii Y, Hashimoto T, Hashizume K** 1997 Inhibition of peroxisome proliferator signaling pathways by thyroid hormone receptor. Competitive binding to the response element. J Biol Chem 272:7752–7758
38. **Irrcher I, Adhihetty PJ, Sheehan T, Joseph AM, Hood DA** 2003 PPARγ coactivator-1α expression during thyroid hormone- and contractile activity-induced mitochondrial adaptations. Am J Physiol Cell Physiol 284:C1669–C1677
39. **van der Putten HH, Friesema EC, Abumrad NA, Everts ME, Visser TJ** 2003 Thyroid hormone transport by the rat fatty acid translocase. Endocrinology 144:1315–1323
40. **Friesema EC, Kuiper GG, Jansen J, Visser TJ, Kester MH** 2006 Thyroid hormone transport by the human monocarboxylate transporter 8 and its rate-limiting role in intracellular metabolism. Mol Endocrinol 20:2761–2772
41. **Habets DD, Coumans WA, Voshol PJ, den Boer MA, Febbraio M, Bonen A, Glatz JF, Luiken JJ** 2007 AMPK-mediated increase in myocardial long-chain fatty acid uptake critically depends on sarcolemmal CD36. Biochem Biophys Res Commun 355:204–210
42. **Boehm EA, Jones BE, Radda GK, Veech RL, Clarke K** 2001 Increased uncoupling proteins and decreased efficiency in palmitate-perfused hyperthyroid rat heart. Am J Physiol Heart Circ Physiol 280:H977–H983
43. **Dummler K, Muller S, Seitz HJ** 1996 Regulation of adenine nucleotide translocase and glycerol 3-phosphate dehydrogenase expression by thyroid hormones in different rat tissues. Biochem J 317(Pt 3):913–918
44. **Jakobsen SN, Hardie DG, Morrice N, Tornqvist HE** 2001 5′-AMP-activated protein kinase phosphorylates IRS-1 on Ser-789 in mouse C2C12 myotubes in response to 5-aminoimidazole-4-carboxamide riboside. J Biol Chem 276:46912–46916
45. **Longnus SL, Ségalen C, Giudicelli J, Sajan MP, Farese RV, Van Obberghen E** 2005 Insulin signalling downstream of protein kinase B is potentiated by 5′AMP-activated protein kinase in rat hearts in vivo. Diabetologia 48:2591–2601
46. **Jessen N, Pold R, Buhl ES, Jensen LS, Schmitz O, Lund S** 2003 Effects of AICAR and exercise on insulin-stimulated glucose uptake, signaling, and GLUT-4 content in rat muscles. J Appl Physiol 94:1373–1379
47. **Fisher JS, Gao J, Han DH, Holloszy JO, Nolte LA** 2002 Activation of AMP kinase enhances sensitivity of muscle glucose transport to insulin. Am J Physiol Endocrinol Metab 282:E18–E23
48. **Carling D, Sanders MJ, Woods A** 2008 The regulation of AMP-activated protein kinase by upstream kinases. Int J Obes (Lond) 32(Suppl 4):S55–S59
49. **Bak MI, Ingwall JS** 1998 Regulation of cardiac AMP-specific 5′-nucleotidase during ischemia mediates ATP resynthesis on reflow. Am J Physiol 274:C992–C1001
50. **Clarke K, Sunn N, Willis RJ** 1989 ^{31}P NMR spectroscopy of hypertrophied rat heart: effect of graded global ischemia. J Mol Cell Cardiol 21:1315–1325
51. **McGee SL, Mustard KJ, Hardie DG, Baar K** 2008 Normal hypertrophy accompanied by phosphoryation and activation of AMP-activated protein kinase α1 following overload in LKB1 knockout mice. J Physiol 586:1731–1741
52. **Yamauchi M, Kambe F, Cao X, Lu X, Kozaki Y, Oiso Y, Seo H** 2008 Thyroid hormone activates adenosine 5′-monophosphate-activated protein kinase via intracellular calcium mobilization and activation of calcium/calmodulin-dependent protein kinase kinase-β. Mol Endocrinol 22:893–903